

**Supplementary Material of**  
**Experimental and theoretical study of**  
**SbPO<sub>4</sub> under compression**

André Luis de Jesus Pereira,<sup>1,2\*</sup> David Santamaría-Pérez,<sup>3</sup> Rosário Vilaplana,<sup>4</sup> Daniel Errandonea,<sup>3</sup> Catalin Popescu,<sup>5</sup> Estelina Lora da Silva,<sup>1</sup> Juan Angel Sans,<sup>1</sup> Juan Rodríguez-Carvajal,<sup>6</sup> Alfonso Muñoz,<sup>7</sup> Plácida Rodríguez-Hernández,<sup>7</sup> Andres Mujica,<sup>7</sup> Silvana Elena Radescu,<sup>7</sup> Armando Beltrán,<sup>8</sup> Alberto Otero de la Roza,<sup>9</sup> Marcelo Nalin,<sup>10</sup> Miguel Mollar,<sup>1</sup> and Francisco Javier Manjón<sup>1\*</sup>

<sup>1</sup> Instituto de Diseño para la Fabricación y Producción Automatizada, MALTA Consolider Team, Universitat Politècnica de València, València, Spain

<sup>2</sup> Grupo de Pesquisa de Materiais Fotonicos e Energia Renovável - MaFER, Universidade Federal da Grande Dourados, Dourados, MS, Brazil

<sup>3</sup> Departament de Física Aplicada – ICMUV, MALTA Consolider Team, Universitat de València, Burjassot, Spain

<sup>4</sup> Centro de Tecnologías Físicas, MALTA Consolider Team, Universitat Politecnica de València, València 46022, Spain

<sup>5</sup> CELLS-ALBA Synchrotron Light Facility, 08290 Cerdanyola, Barcelona, Spain

<sup>6</sup> Institut Laue-Langevin, 71 Avenue des Martyrs, CS 20156, 38042, Grenoble, Cedex 9, France

<sup>7</sup> Departamento de Física, Instituto de Materiales y Nanotecnología, MALTA Consolider Team, Universidad de La Laguna, Tenerife, Spain

<sup>8</sup> Departament de Química Física, MALTA Consolider Team, Universitat de València, 46100 Burjassot, Spain

<sup>9</sup> Departamento de Química Física y Analítica, MALTA Consolider Team, Universidad de Oviedo, 33006 Oviedo, Spain

<sup>10</sup> Instituto de Química, Depto. Química Geral e Inorgânica, UNESP - Campus de Araraquara, SP, Brazil

**Structural and Vibrational Properties at Room Pressure**

**Table S1.** Theoretical atomic coordinates of the monoclinic  $P2_1/m$  (space group Nr. 11) structure of SbPO<sub>4</sub> at room conditions. Lattice parameters are:  $a = 5.0482 \text{ \AA}$ ,  $b = 6.8228 \text{ \AA}$ ,  $c = 4.7392 \text{ \AA}$  and  $\beta = 97.0624^\circ$ , with a unit cell volume  $V_0 = 161.9968 \text{ \AA}^3$ .

Atom	Wyckoff position	x	y	z
Sb	2e	0.16677	0.25	0.18534
P	2e	0.61036	0.25	0.72021
O1	2e	0.32278	0.25	0.81191
O2	2e	0.55847	0.25	0.38998
O3	4f	0.77615	0.07144	0.83277

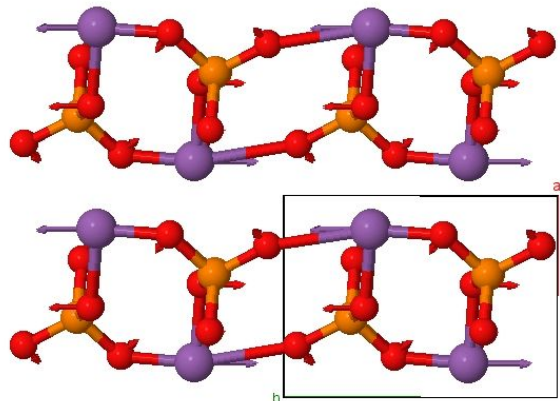


**Figure S1.** Atomic vibrations (along the  $b$ -axis) of the  $B_g$  mode of  $75\text{ cm}^{-1}$ , which is one of the shear layer modes of  $\text{SbPO}_4$ . Sb (big purple), P (medium-size orange) and O (small red).

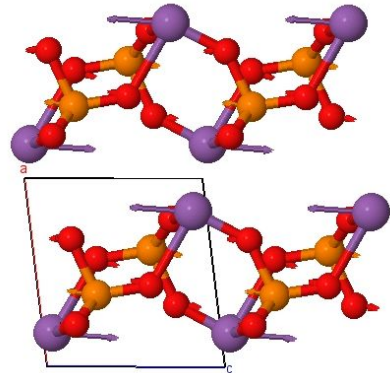


**Figure S2.** Atomic vibrations (along the  $c$ -axis) of the  $A_g$  mode of  $89\text{ cm}^{-1}$ , which is one of the shear layer modes of  $\text{SbPO}_4$ . Sb (big purple), P (medium-size orange) and O (small red).

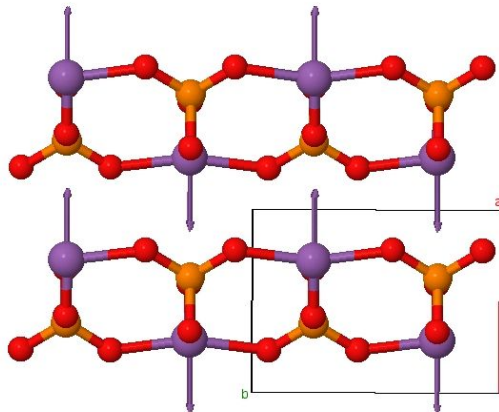


**Figure S3.** Atomic vibrations (along the  $a$ -axis) of the  $A_g$  mode of  $106\text{ cm}^{-1}$ , which is the main longitudinal layer mode of SbPO<sub>4</sub>. Sb (big purple), P (medium-size orange) and O (small red).

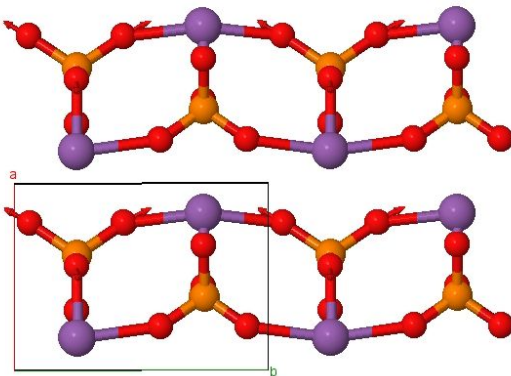


**Figure S4.** Atomic vibrations (mainly of O atoms) of the  $A_g$  mode of  $936\text{ cm}^{-1}$ , which is the symmetric stretching mode of PO<sub>4</sub> in SbPO<sub>4</sub>. Sb (big purple), P (medium-size orange) and O (small red).

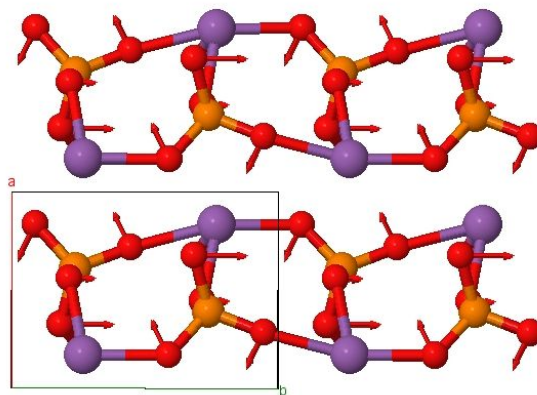


**Figure S5.** Atomic vibrations of the  $A_u$  mode of  $220\text{ cm}^{-1}$ , which is the main rotational mode of  $\text{PO}_4$  in  $\text{SbPO}_4$ . Sb (big purple), P (medium-size orange) and O (small red).

### Structural properties of $\text{SbPO}_4$ at high pressure

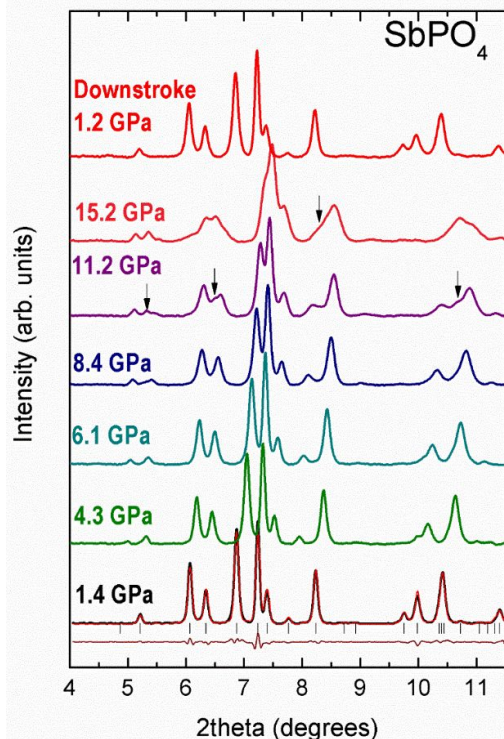


**Figure S6.** Angle-dispersive XRD of  $\text{SbPO}_4$  measured at different pressures up to  $15.2\text{ GPa}$  at room temperature. In order to facilitate the identification of changes in the XRD pattern related to the phase transition we represent  $2\theta < 11.5^\circ$ ; i.e. the part of the XRD without overlapping with Cu or gasket peaks. The top pattern corresponds to the recovered sample at  $1.2\text{ GPa}$  after decompression from  $15.2\text{ GPa}$ . The black arrows indicate the position of new peaks not related to the initial phase.

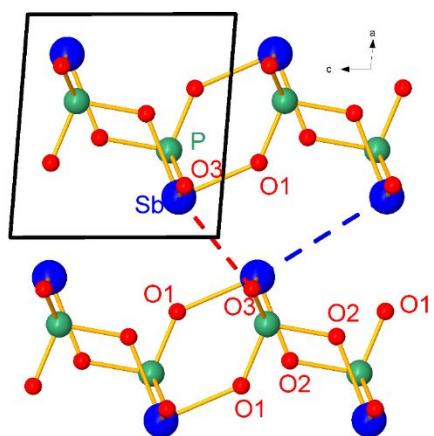


**Figure S7.** Detail of the monoclinic structure of  $\text{SbPO}_4$  along the  $ac$ -plane. The directions of maximum and intermediate compressibility at room pressure are approximately along the plotted dashed red and blue lines, respectively.

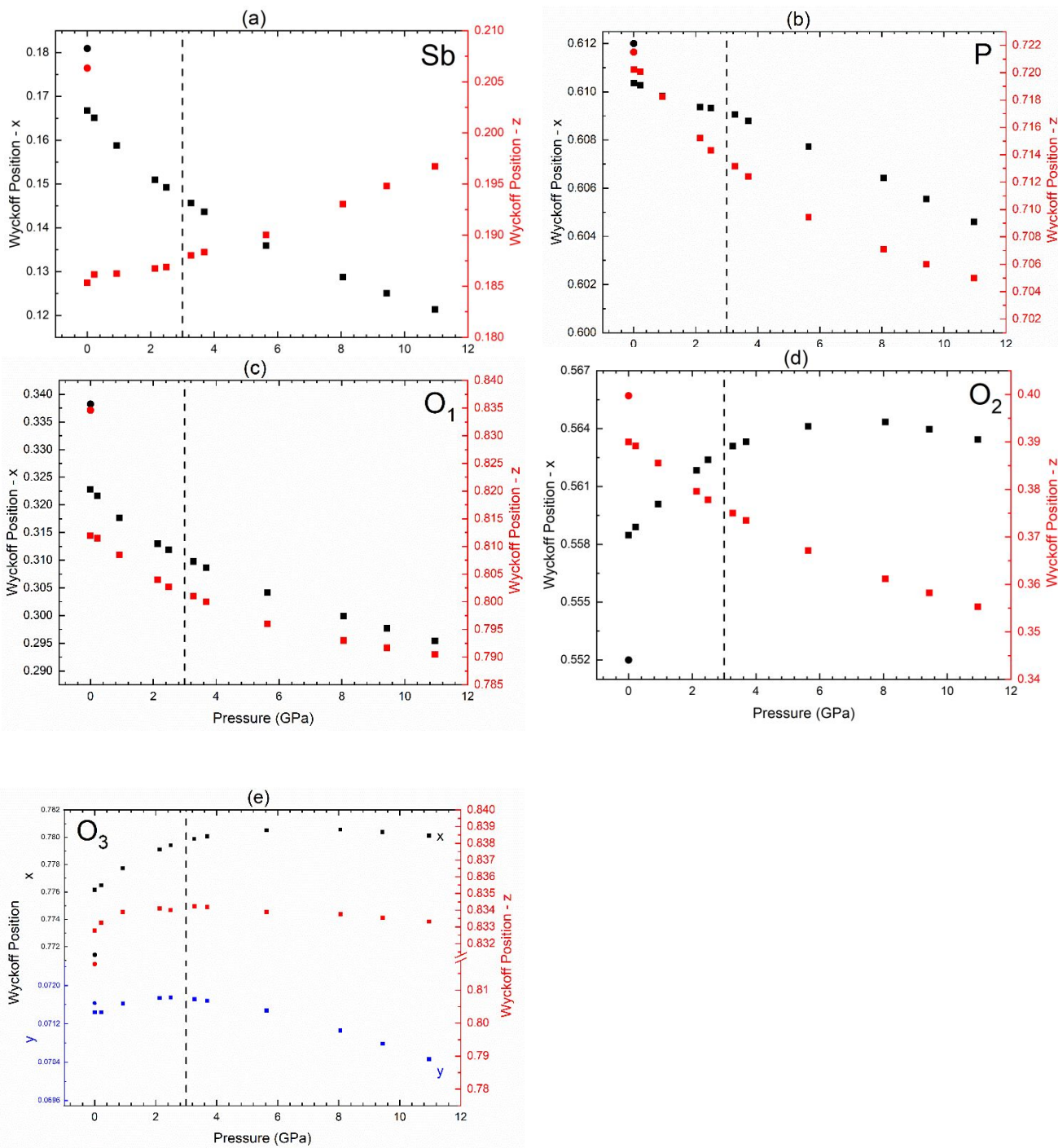


**Figure S8.** Evolution of the theoretical Wyckoff positions of monoclinic  $\text{SbPO}_4$  with pressure (squares). The circles represent the experimental positions obtained by the Rietveld refinement of the XRD measurement performed at room pressure. The vertical dashed lines at 3 GPa indicate the pressure at which the IPT occurs as suggested by the change of the tendency of many Wyckoff coordinates.

**Table S2.** Theoretical (GGA-PBESol) atomic coordinates of proposed triclinic *P*-1 (space group Nr. 2) structure of SbPO<sub>4</sub> at 15.005 GPa. Lattice parameters are:  $a = 4.3335 \text{ \AA}$ ,  $b = 4.7040 \text{ \AA}$ ,  $c = 6.5659 \text{ \AA}$ ,  $\alpha = 89.8023^\circ$ ,  $\beta = 89.6317^\circ$ , and  $\gamma = 85.3338^\circ$ , with a unit cell volume  $V_0 = 133.3999 \text{ \AA}^3$ .

Atom	Wyckoff position	x	y	z
Sb	2i	0.79835	0.11293	0.75058
P	2i	0.29724	0.60217	0.74951
O1	2i	0.21180	0.29039	0.74841
O2	2i	0.65143	0.56153	0.74953
O3	2i	0.16606	0.77782	-0.06971
O4	2i	0.83102	0.21922	0.43054

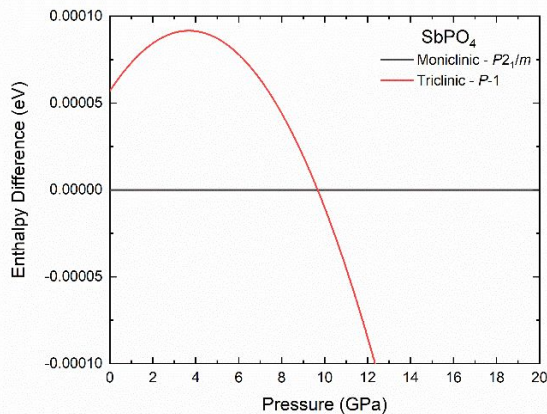


**Figure S9.** Theoretical enthalpy difference vs pressure of the triclinic HP phase of SbPO<sub>4</sub> (red line) with respect to the monoclinic LP phase (black line).

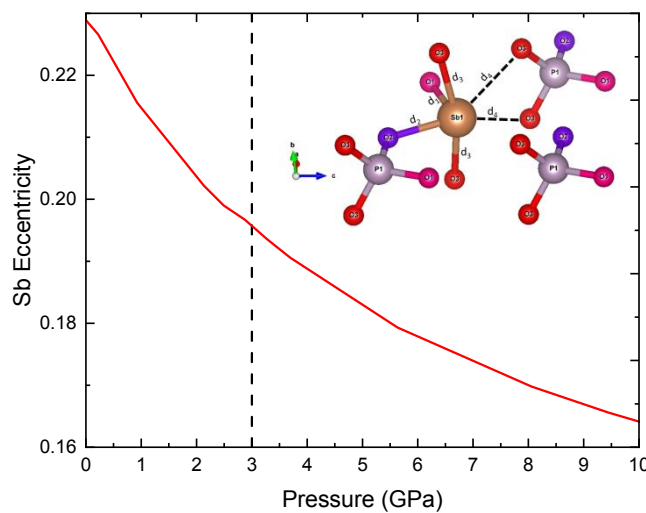


**Figure S10.** Pressure dependence of the theoretical Sb eccentricity in the SbO<sub>6</sub> polyhedron of monoclinic SbPO<sub>4</sub>. The Sb eccentricity was calculated using the IVTON software<sup>1</sup>.

## Vibrational properties of SbPO<sub>4</sub> at high pressure

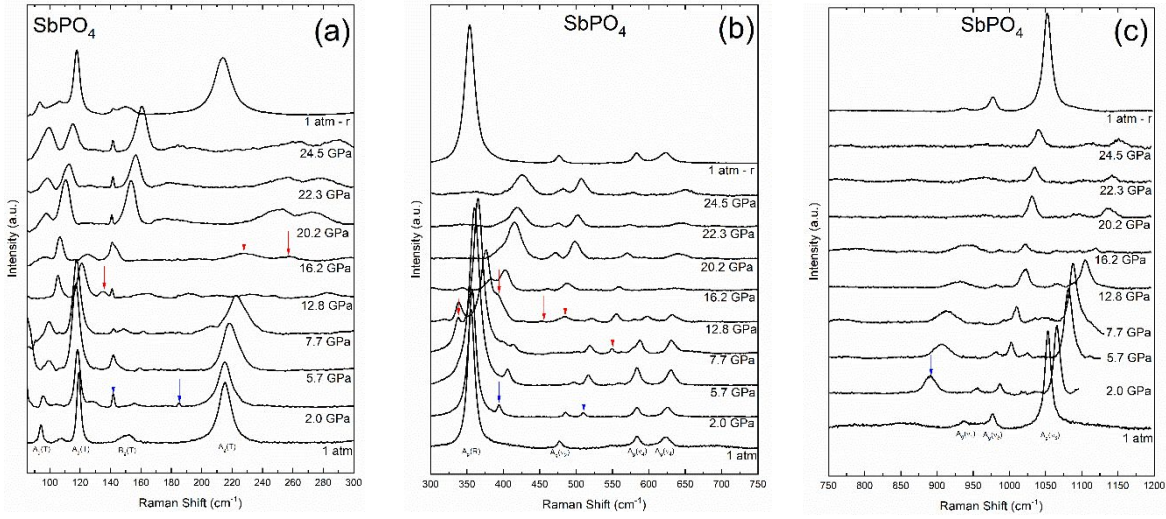


**Figure S11.** Room-temperature Raman spectra of SbPO<sub>4</sub> at selected pressures up to 24.5 GPa. (a) Low-frequency region, (b) Middle-frequency region, and (c) High-frequency region. Top Raman spectrum corresponds to the recovered sample after decompression from 24.5 GPa. Red arrows indicate the position of new peaks not related to the initial phase and blue arrows indicate peaks that either are not related to the sample or correspond to second-order modes of the original sample (see main text). In the bottom of the figures we have added a tentative mode assignment of the initial sample based in the theoretical results and the pressure evolution of these vibrational modes. Notations T, R, v<sub>1</sub>, v<sub>2</sub>, v<sub>3</sub>, and v<sub>4</sub> refer to the main character of translation, rotation, or internal modes of the PO<sub>4</sub> units, respectively.

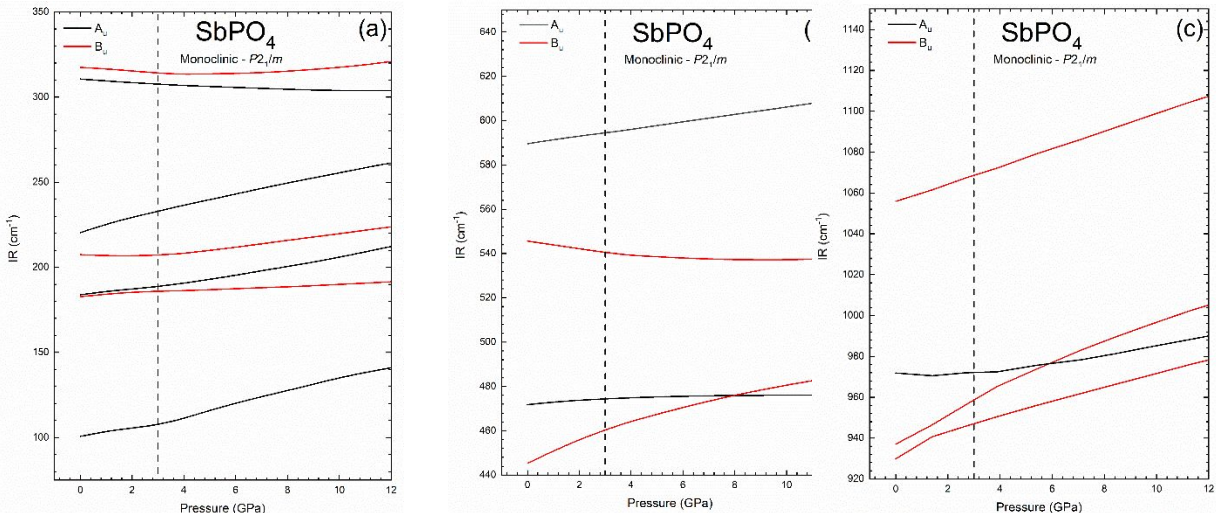


**Figure S12.** Theoretical pressure dependence of the IR-active modes of monoclinic SbPO<sub>4</sub>: (a) from 75 to 350 cm<sup>-1</sup>; (b) from 440 to 620 cm<sup>-1</sup>, (c) from 920 to 1150 cm<sup>-1</sup>. The vertical dashed lines at 3 GPa indicate the pressure at which the IPT occurs as suggested by the change of many frequency pressure coefficients.

**Table S3.** Theoretical IR-active mode frequencies and pressure coefficients of monoclinic  $\text{SbPO}_4$  obtained by fitting the equation  $\omega(P) = \omega_0 + a \cdot P$  up to 3 GPa.

Symmetry	Theoretical	
	$\omega_0$ (cm <sup>-1</sup> )	$a$ (cm <sup>-1</sup> /GPa)
$A_u(T)$	101(2)	2.2(4)
$B_u(T)$	183(2)	1.2(2)
$A_u(R)$	184(2)	1.6(2)
$B_u(T)$	207(3)	-0.2(2)
$A_u(R)$	220(3)	4.2(4)
$A_u(v_2)$	311(4)	-1.1(1)
$B_u(R)$	317(4)	-1.1(1)
$B_u(v_2)$	445(5)	5.2(2)
$A_u(v_4)$	472(5)	0.9(1)
$B_u(v_4)$	546(6)	-1.7(1)
$B_u(v_4)$	589(6)	1.7(1)
$B_u(v_3)$	930(8)	6.0(1.0)
$B_u(v_1)$	937(8)	7.2(3)
$A_u(v_3)$	972(8)	0.04(0.60)
$B_u(v_3)$	1056(9)	4.3(2)

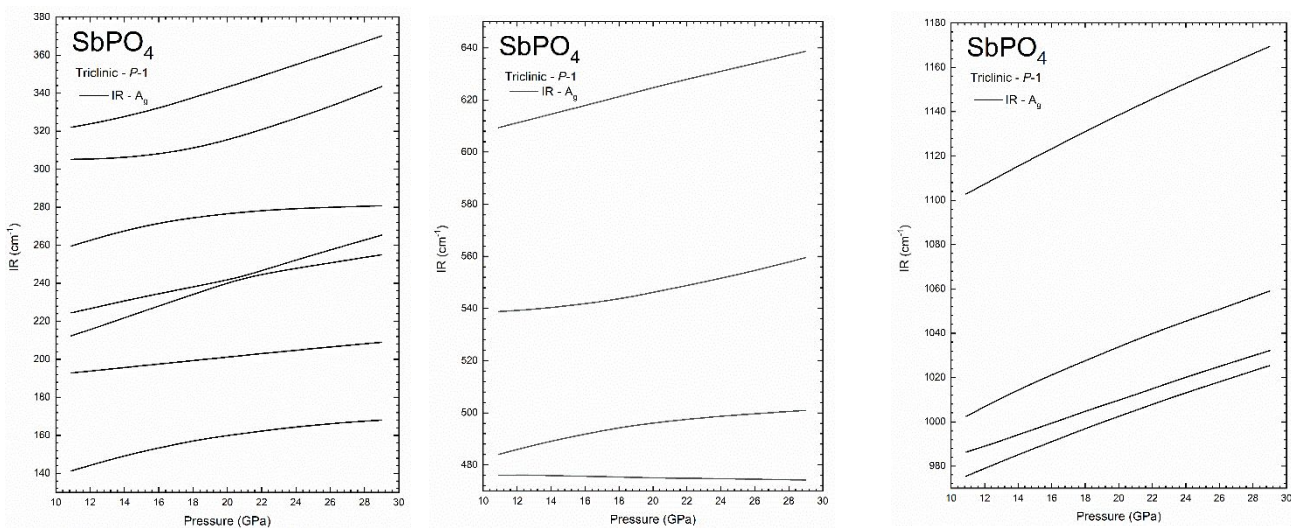


**Figure S13.** Pressure dependence of the theoretical IR-active modes of the triclinic HP ( $P-1$ ) phase of  $\text{SbPO}_4$ : (a) from 130 to 380 cm<sup>-1</sup>; (b) from 470 to 650 cm<sup>-1</sup>, (c) from 970 to 1180 cm<sup>-1</sup>.

**Table S4.** Theoretical IR-active mode frequencies and pressure coefficients of the triclinic HP ( $P-1$ ) phase of  $\text{SbPO}_4$  obtained by fitting the equation  $\omega(P) = \omega_{10.9\text{GPa}} + a \cdot P$  from 10.9 GPa up to 14 GPa.

Symmetry	Theoretical	
	$\omega_{10.9\text{GPa}}$ (cm $^{-1}$ )	$a$ (cm $^{-1}$ /GPa)
A <sub>u</sub>	141.3	2.53
A <sub>u</sub>	192.8	0.91
A <sub>u</sub>	212.3	3.07
A <sub>u</sub>	224.4	2.03
A <sub>u</sub>	259.6	2.56
A <sub>u</sub>	305.2	0.36
A <sub>u</sub>	322.1	1.83
A <sub>u</sub>	476.0	-0.04
A <sub>u</sub>	484.0	1.63
A <sub>u</sub>	538.8	0.52
A <sub>u</sub>	609.4	1.66
A <sub>u</sub>	975.5	3.11
A <sub>u</sub>	986.4	2.55
A <sub>u</sub>	1002.4	3.82
A <sub>u</sub>	1102.9	4.06

**Table S5.** Sb-O distances, charge density, and its Laplacian at the BCPs of the different Sb-O distances calculated at different pressures for the monoclinic and triclinic phases of  $\text{SbPO}_4$ .

distance	$l(\text{Sb-O}) [\text{\AA}]$	$\rho(\mathbf{r}) [\text{A.U.}]$	$\nabla^2\rho(\mathbf{r}) [\text{A.U.}]$
Monoclinic 0 GPa			
d <sub>1</sub>	2.02339	0.11079	0.37097
d <sub>2</sub>	2.09001	0.09763	0.27354
d <sub>3</sub> (x2)	2.21486	0.07231	0.16590
d <sub>4</sub> (x2)	2.72456	0.02811	0.06543
d <sub>6</sub>	3.35994	0.00915	0.02447
Monoclinic 1.9 GPa			
d <sub>1</sub>	2.02878	0.10964	0.30392
d <sub>2</sub>	2.11659	0.09261	0.23692
d <sub>3</sub> (x2)	2.21421	0.07231	0.16348
d <sub>4</sub> (x2)	2.61149	0.03483	0.07713
d <sub>6</sub>	3.12937	0.01403	0.03199

	Monoclinic 2.6 GPa		
d <sub>1</sub>	2.03018	0.10933	0.28307
d <sub>2</sub>	2.12284	0.09146	0.25143
d <sub>3</sub> (x2)	2.21295	0.07246	0.16420
d <sub>4</sub> (x2)	2.58776	0.03645	0.08129
d <sub>6</sub>	3.08092	0.01534	0.03579
	Monoclinic 3.5 GPa		
d <sub>1</sub>	2.03136	0.10906	0.28190
d <sub>2</sub>	2.12786	0.09056	0.16683
d <sub>3</sub> (x2)	2.21006	0.07286	0.16658
d <sub>4</sub> (x2)	2.56892	0.03777	0.08368
d <sub>5</sub>	2.82774	0.02322	0.07290
d <sub>6</sub>	3.03545	0.01669	0.04056
	Monoclinic 4.4 GPa		
d <sub>1</sub>	2.03257	0.10877	0.27837
d <sub>2</sub>	2.13330	0.08957	0.18874
d <sub>3</sub> (x2)	2.20692	0.07330	0.16912
d <sub>4</sub> (x2)	2.54936	0.03921	0.08624
d <sub>5</sub>	2.80201	0.02434	0.07734
d <sub>6</sub>	2.99071	0.01813	0.04496
	Monoclinic 5.4 GPa		
d <sub>1</sub>	2.03317	0.10861	0.27036
d <sub>2</sub>	2.13794	0.08871	0.21201
d <sub>3</sub> (x2)	2.20384	0.07372	0.17080
d <sub>4</sub> (x2)	2.53247	0.04050	0.08879
d <sub>5</sub>	2.77898	0.02544	0.07566
d <sub>6</sub>	2.94995	0.01956	0.05080
	Triclinic 9.2 GPa		
d <sub>1</sub>	2.03632	0.10780	0.27534
d <sub>2</sub>	2.14858	0.08681	0.23149
d <sub>3</sub>	2.18742	0.07614	0.18776
d <sub>4</sub>	2.19111	0.07553	0.17683

$d_5$	2.48779	0.04410	0.09570
$d_6$	2.49095	0.04389	0.10101
$d_7$	2.69777	0.02975	0.08474
$d_8$	2.83082	0.02444	0.06802
Triclinic 14.8 GPa			
$d_1$	2.03757	0.10734	0.30906
$d_2$	2.15416	0.08580	0.21052
$d_3$	2.16514	0.07958	0.21339
$d_4$	2.16902	0.07892	0.19852
$d_5$	2.45254	0.04716	0.10237
$d_6$	2.45335	0.04716	0.10157
$d_7$	2.61003	0.03529	0.08232
$d_8$	2.72048	0.03012	0.07075
Triclinic 20.6 GPa			
$d_1$	2.03722	0.10725	0.32829
$d_2$	2.15371	0.08585	0.20428
$d_3$	2.14647	0.08257	0.25353
$d_4$	2.14654	0.08254	0.25425
$d_5$	2.42827	0.04946	0.11156
$d_6$	2.43038	0.04926	0.11073
$d_7$	2.53880	0.04048	0.09595
$d_8$	2.64415	0.03485	0.09446

## **References**

- (1) Balić Žunić, T.; Vicković, I. IVTON - Program for the Calculation of Geometrical Aspects of Crystal Structures and Some Crystal Chemical Applications. *J. Appl. Crystallogr.* **1996**, *29* (1), 305–306. <https://doi.org/10.1107/s0021889895015081>.